

Measurements of CP Violation, Mixing and Lifetimes of B Mesons with the *BABAR* Detector

Sören Prell

University of California at San Diego

Department of Physics

9500 Gilman Drive, La Jolla, CA 92093

(for the *BABAR* Collaboration)

Abstract

We report the observation of CP violation in the B^0 meson system. Using a novel technique for time-dependent measurements, we measure a non-zero value for the CP -violating amplitude $\sin 2\beta$ at the 4.1σ level. We also report on precision measurements of the B^+ and B^0 lifetimes and the $B^0\bar{B}^0$ mixing frequency Δm_d obtained with the same technique, and on a first measurement of the time-dependent CP -violating amplitude in $B^0 \rightarrow \pi^+\pi^-$ decays.

Contributed to the Proceedings of the
9th International Symposium on Heavy Flavor Physics,
9/10/2001—9/13/2001, Caltech, Pasadena

Stanford Linear Accelerator Center, Stanford University, Stanford, CA 94309

Work supported in part by Department of Energy contract DE-AC03-76SF00515.

1 Introduction

CP violation has been a central concern of particle physics since its discovery in 1964 in the decays of K_L^0 mesons [1]. An elegant explanation of the origin of CP violation was proposed by Kobayashi and Maskawa, as a complex phase in the three-generation CKM quark-mixing matrix [2]. In this picture, measurements of CP -violating asymmetries in the time distributions of B^0 decays to charmonium final states are expected to be large and provide a direct test of the Standard Model of electroweak interactions [3].

We present measurements of time-dependent CP -asymmetries in samples of fully reconstructed B decays to charmonium-containing CP eigenstates ($b \rightarrow c\bar{c}s$) and to the $\pi^+\pi^-$ final state. The data for these studies were recorded at the $\Upsilon(4S)$ resonance by the BABAR detector at the PEP-II asymmetric-energy e^+e^- collider at the Stanford Linear Accelerator Center.

When the $\Upsilon(4S)$ decays, the P -wave $B^0\bar{B}^0$ state evolves coherently until one of the mesons decays. In one of four time-order and flavor configurations, if the tagging meson B_{tag} decays first, and as a B^0 , the other meson must be a \bar{B}^0 at that same time t_{tag} . It then evolves independently, and can decay into a CP eigenstate B_{CP} at a later time t_{CP} . The time between the two decays $\Delta t = t_{CP} - t_{\text{tag}}$ is a signed quantity made measurable by producing the $\Upsilon(4S)$ with a boost $\beta\gamma = 0.56$ along the collision (z) axis, with nominal energies of 9.0 and 3.1 GeV for the electron and positron beams. The measured distance $\Delta z \approx \beta\gamma c\Delta t$ between the two decay vertices provides a good estimate of the corresponding time interval Δt ; the average value of $|\Delta z|$ is $\beta\gamma c\tau_{B^0} \approx 250 \mu\text{m}$.

We examine each of the events in the B_{CP} sample for evidence that the other neutral B meson decayed as a B^0 or a \bar{B}^0 (flavor tag). The distribution $f_+(f_-)$ of the decay rate when the tagging meson is a $B^0(\bar{B}^0)$ is given by

$$f_{\pm}(\Delta t) = \frac{e^{-|\Delta t|/\tau}}{4\tau} [1 \pm S \sin(\Delta m_d \Delta t) \mp C \cos(\Delta m_d \Delta t)], \quad (1)$$

where Δt is the time between the two B decays, τ is the B^0 lifetime [4], Δm_d is the $B^0\bar{B}^0$ mixing frequency [4], and the lifetime difference between neutral B mass eigenstates is assumed to be negligible. The sine term in Eq. 1 is due to interference between direct decay and decay after mixing, and the cosine term is due to direct CP violation. The CP -violating parameters S and C are defined in terms of a complex parameter λ that depends on both $B^0\bar{B}^0$ mixing and on the amplitudes describing \bar{B}^0 and B^0 decay to a common final state f [5]:

$$S = \frac{2 \mathcal{I}m\lambda}{1 + |\lambda|^2} \quad \text{and} \quad C = \frac{1 - |\lambda|^2}{1 + |\lambda|^2}. \quad (2)$$

A difference between the B^0 and \bar{B}^0 Δt distributions or a Δt asymmetry for either flavor tag is evidence for CP violation.

In the Standard Model $\lambda = \eta_f e^{-2i\beta}$ for charmonium-containing $b \rightarrow c\bar{c}s$ decays, η_f is the CP eigenvalue of the state f and $\beta = \arg[-V_{cd}V_{cb}^*/V_{td}V_{tb}^*]$ is an angle of the Unitarity Triangle of the three-generation CKM matrix [2]. Thus, the time-dependent CP -violating asymmetry is

$$A_{CP}(\Delta t) \equiv \frac{f_+(\Delta t) - f_-(\Delta t)}{f_+(\Delta t) + f_-(\Delta t)} = -\eta_f \sin 2\beta \sin(\Delta m_{B^0} \Delta t). \quad (3)$$

The analogous time-dependent CP -violating asymmetry in the decay $B^0 \rightarrow \pi^+\pi^-$ arises from interference between mixing and decay amplitudes, and interference between the $b \rightarrow uW^-$ (tree) and $b \rightarrow dg$ (penguin) decay amplitudes. If the decay proceeds purely through the tree process, the complex parameter λ is directly related to CKM matrix elements and $|\lambda| = 1$ and $\mathcal{I}m\lambda = \sin 2\alpha$, where $\alpha = \arg[-V_{td}V_{tb}^*/V_{ud}V_{ub}^*]$.

However, recent theoretical estimates suggest that the contribution from the gluonic penguin amplitude can be significant [6] leading to $|\lambda| \neq 1$ and $\mathcal{I}m\lambda = |\lambda| \sin 2\alpha_{\text{eff}}$, where α_{eff} depends on the magnitudes and strong phases of the tree and penguin amplitudes.

We also present precise measurements of the B^0 - \bar{B}^0 mixing frequency Δm_d and the neutral and charged B lifetimes. These measurements use the same vertexing algorithm and Δt calculation as the measurements of the CP -asymmetries. In addition, for the Δm_d measurement, the same flavor tagging algorithm as for the CP analyses is used. These measurements are amongst the most precise available and provide a good validation of the novel technique to study time-dependent B decays.

In all analyses the values of the parameters under study (B lifetimes, Δm_d , $\sin 2\beta$, $S_{\pi\pi}$ and $C_{\pi\pi}$) were hidden to eliminate possible experimenter's bias until event selection, Δt reconstruction method, and fitting procedures were finalized and systematic errors were determined.

2 The *BABAR* Detector

A detailed description of the *BABAR* detector can be found in Ref. [7]. Charged particles are detected and their momenta measured by a combination of a silicon vertex tracker (SVT) consisting of five double-sided layers and a central drift chamber (DCH), in a 1.5-T solenoidal field. The average vertex resolution in the z direction is $70 \mu\text{m}$ for a fully reconstructed B meson. We identify leptons and hadrons with measurements from all detector systems, including the energy loss (dE/dx) in the DCH and SVT. Electrons and photons are identified by a CsI electromagnetic calorimeter (EMC). Muons are identified in the instrumented flux return (IFR). A Cherenkov ring imaging detector (DIRC) covering the central region, together with the dE/dx information, provides K - π separation of at least three standard deviations for B decay products with momentum greater than $250 \text{ MeV}/c$ in the laboratory.

3 Measurement of B Lifetimes and Δm_d

The measurements of the charged and neutral B lifetimes and the B^0 - \bar{B}^0 mixing frequency Δm_d are based on a sample of approximately 23 million $B\bar{B}$ pairs.

3.1 Exclusive B Reconstruction

Samples of B^0 and B^+ mesons B_{rec} are reconstructed in the modes $B^0 \rightarrow D^{(*)-}\pi^+$, $D^{(*)-}\rho^+$, $D^{(*)-}a_1^+$, $J/\psi K^{*0}$ and $B^+ \rightarrow \bar{D}^{(*)0}\pi^+$, $J/\psi K^+$, $\psi(2S)K^+$. Charged and neutral \bar{D}^* candidates are formed by combining a \bar{D}^0 with a π^- or π^0 . \bar{D}^0 candidates are reconstructed in the decay channels $K^+\pi^-$, $K^+\pi^-\pi^0$, $K^+\pi^+\pi^-\pi^-$ and $K_s^0\pi^+\pi^-$ and D^- candidates in the decay channels $K^+\pi^-\pi^-$ and $K_s^0\pi^-$. We reconstruct J/ψ and $\psi(2S)$ in the decays to e^+e^- and $\mu^+\mu^-$ and the $\psi(2S)$ decay to $J/\psi \pi^+ \pi^-$.

Continuum $e^+e^- \rightarrow q\bar{q}$ background is suppressed by requirements on the normalized second Fox-Wolfram moment [8] for the event and on the angle between the thrust axes of B_{rec} and of the other $B = B_{\text{opp}}$ in the event. B candidates are identified by the difference ΔE between the reconstructed B energy and the beam energy $\sqrt{s}/2$ in the $\Upsilon(4S)$ frame, and the beam-energy substituted mass m_{ES} calculated from $\sqrt{s}/2$ and the reconstructed B momentum. We require $m_{\text{ES}} > 5.2 \text{ GeV}/c^2$ and $|\Delta E| < 3\sigma_{\Delta E}$. The distributions of m_{ES} for selected B candidates in 30 fb^{-1} is shown in Fig. 3.1.

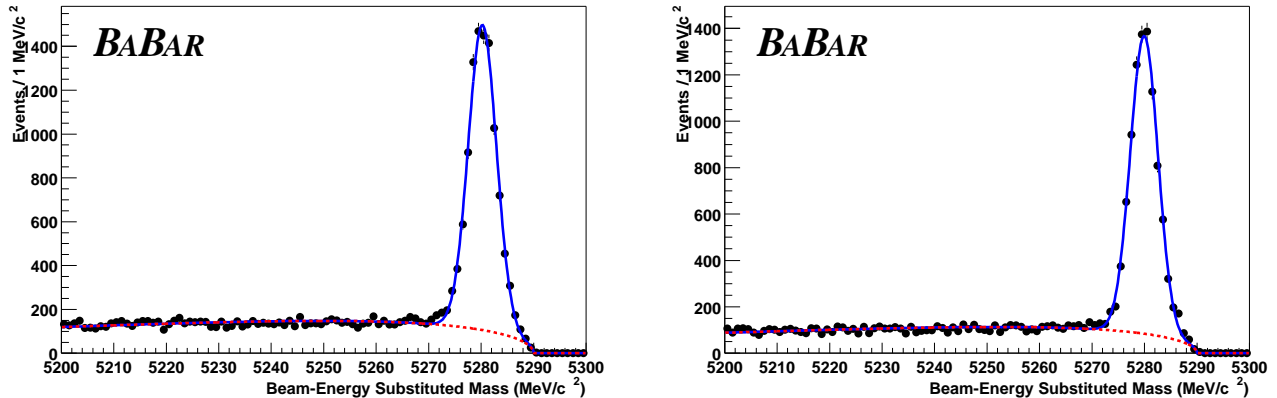


Figure 1: Beam energy substituted mass distribution for selected B^0 (left) and B^+ (right) candidates. In 30 fb^{-1} , we reconstruct 9400 B^0 and 8500 B^+ signal events. Average signal purities for $m_{\text{ES}} > 5.27 \text{ GeV}/c^2$, are 83 % and 85 % for B^0 and B^+ , respectively.

3.2 Δt Measurement

The decay time difference, Δt , between B decays is determined from the measured separation $\Delta z = z_{\text{rec}} - z_{\text{opp}}$ along the z axis between the B_{rec} and the B_{opp} vertices. This Δz is converted into Δt using the $\Upsilon(4S)$ boost and correcting on an event-by-event basis for the direction of the B mesons. The resolution of the Δt measurement is dominated by the z resolution of the B_{opp} decay vertex. This vertex uses all tracks in the event except those incorporated in B_{rec} . An additional constraint is provided by a calculated B_{opp} production point and three-momentum, determined from the three-momentum of the B_{rec} candidate, its decay vertex, and the average position of the interaction point and the $\Upsilon(4S)$ boost. Reconstructed K_S^0 or Λ candidates are used as input to the fit in place of their daughters in order to reduce bias due to long-lived particles. Tracks with a large contribution to the χ^2 are iteratively removed from the fit, until all remaining tracks have a reasonable fit probability. Candidates with $|\Delta z| < 3.0 \text{ mm}$ and $\sigma_{\Delta z} < 400 \mu\text{m}$ are retained. For the measurement of the B lifetimes, we require that at least two tracks are included in the B_{opp} vertex.

Two different parameterizations are used to model the decay-time difference resolution functions. In the measurements of Δm_d , $\sin 2\beta$, and $\sin 2\alpha$, the resolution function is approxi-

mated by a sum of three Gaussian distributions with different means δ_k and widths σ_k ,

$$\mathcal{R}(\delta_t, \sigma_{\Delta t} | \hat{a}) = \sum_{k=1}^3 \frac{f_k}{\sigma_k \sqrt{2\pi}} e^{-(\delta_t - \delta_k)^2 / 2\sigma_k^2}, \quad (4)$$

where δ_t is the difference between the measured and true Δt values. For the core and tail Gaussians, the widths $\sigma_{1,2} = S_{1,2} \times \sigma_{\Delta t}$ are the scaled event-by-event measurement error, $\sigma_{\Delta t}$, derived from the vertex fits. The third Gaussian, with a fixed width of $\sigma_3 = 8$ ps, accounts for less than 1% of *outlier* events with incorrectly reconstructed vertices. The three Gaussian resolution function is not suited for the measurement of the B lifetimes because strong correlations lead to increased statistical errors. Studies with Monte Carlo simulation and data show that the sum of a zero-mean Gaussian distribution and its convolution with an exponential provides a good trade-off between statistical and systematic uncertainties:

$$\begin{aligned} \mathcal{R}(\delta_t, \sigma_{\Delta t} | \hat{a} = \{h, s, \kappa\}) &= h \frac{1}{\sqrt{2\pi} s \sigma_{\Delta t}} \exp\left(-\frac{\delta_t^2}{2s^2 \sigma_{\Delta t}^2}\right) \\ &+ \int_{-\infty}^0 \frac{1-h}{\kappa \sigma_{\Delta t}} \exp\left(\frac{\delta'_t}{\kappa \sigma_{\Delta t}}\right) \frac{1}{\sqrt{2\pi} s \sigma_{\Delta t}} \exp\left(-\frac{(\delta_t - \delta'_t)^2}{2s^2 \sigma_{\Delta t}^2}\right) d(\delta'_t). \end{aligned} \quad (5)$$

The parameters \hat{a} are the fraction h in the core Gaussian component, a scale factor s for the per-event errors $\sigma_{\Delta t}$, and the factor κ in the effective time constant $\kappa \sigma_{\Delta t}$ of the exponential which accounts for charm decays. Δt *outlier* events are modeled the same way as in the three Gaussian resolution function. The resolution function parameters are assumed to be the same for all B^0 and B^+ decay modes. This assumption is confirmed by Monte Carlo simulation studies. The resolution functions differ only slightly between B^0 and B^+ mesons due to different mixtures of D^- and \bar{D}^0 mesons in the B_{opp} decays and we use a single set of resolution function parameters for both B^0 and B^+ in the lifetime fits.

3.3 B Lifetime Results

We extract the B^+ and B^0 lifetimes from an unbinned maximum likelihood fit to the Δt distributions of the selected B candidates. The probability for an event to be signal is estimated from m_{ES} fits (Fig. 3.1) and the m_{ES} value of the B_{rec} candidate. In the likelihood, the probability density for the signal events is given by

$$\mathcal{G}(\Delta t, \sigma_{\Delta t} | \tau, \hat{a}) = \int_{-\infty}^{+\infty} e^{-|\Delta t|/\tau} / (2\tau) \mathcal{R}(\Delta t - \Delta t', \sigma_{\Delta t} | \hat{a}) d(\Delta t'), \quad (6)$$

and the background Δt distribution for each B species is empirically modeled by the sum of a prompt component and a lifetime component convolved with the same resolution function, but with a separate set of parameters. The likelihood fit involves 17 free parameters in addition to the B^0 and the B^+ lifetimes: 12 to describe the background Δt distributions and 5 for the signal resolution function. The charged B lifetime τ_{B^+} is replaced with $\tau_{B^+} = r \cdot \tau_{B^0}$ to estimate the statistical error on the ratio $r = \tau_{B^+} / \tau_{B^0}$.

We determine the B^0 and B^+ meson lifetimes and their ratio to be:

$$\begin{aligned} \tau_{B^0} &= 1.546 \pm 0.032 \text{ (stat)} \pm 0.022 \text{ (syst)} \text{ ps}, \\ \tau_{B^+} &= 1.673 \pm 0.032 \text{ (stat)} \pm 0.023 \text{ (syst)} \text{ ps, and} \\ \tau_{B^+} / \tau_{B^0} &= 1.082 \pm 0.026 \text{ (stat)} \pm 0.012 \text{ (syst)}. \end{aligned}$$

These are the most precise measurements to date [9] and are consistent with the world averages [4]. The resolution function parameters are consistent with those found in a Monte Carlo simulation that includes detector alignment effects. Figure 3.3 shows the results of the likelihood fit superimposed on the Δt distributions for B^0 and B^+ events. With the current data sample these measurements are still statistically limited. The dominant systematic errors arise from uncertainties in the description of the combinatorial background and of events with large Δt values, the use of a common time resolution function for B^0 and B^+ and from limited Monte Carlo statistics.

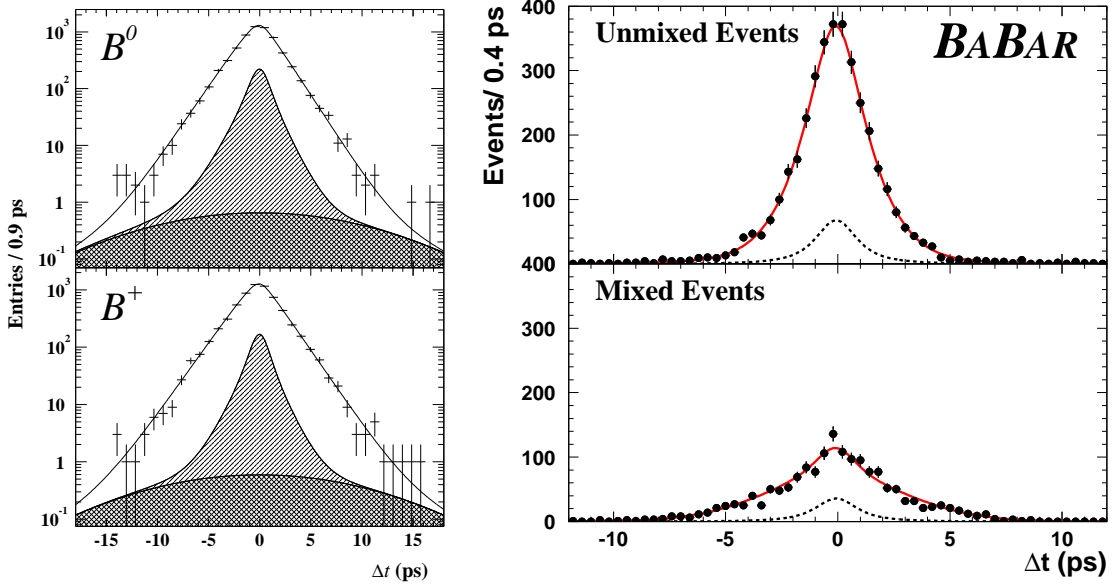


Figure 2: Left: Δt distribution for the B^0 (top) and B^+ (bottom) events within 2σ of the B mass with superimposed fit results. The single-hatched areas are the background contributions and the cross-hatched areas represent the Δt outliers. The probability of obtaining a lower likelihood is 7.3%. Right: Δt distributions in data for the mixed and unmixed events ($m_{ES}(B_{rec}) > 5.27 \text{ GeV}/c^2$), with overlaid the projection of the likelihood fit (solid) and the background contributions (dashed).

3.4 B Flavor Tagging

The measurements of Δm_d , $\sin 2\beta$ and $\sin 2\alpha$ require knowledge of the $B_{\text{opp}} = B_{\text{tag}}$ flavor. We use the same tagging algorithm in the three analyses to determine the B_{tag} flavor from the charges of its decay products.

The charge of energetic electrons and muons from semileptonic B decays, kaons, soft pions from D^* decays, and high momentum charged particles is correlated with the flavor of the decaying b quark. Each event is assigned to one of four hierarchical, mutually exclusive tagging categories or has no flavor tag. A lepton tag requires an electron (muon) candidate with a center-of-mass momentum $p_{\text{cm}} > 1.0$ (1.1) GeV/c . This efficiently selects primary leptons and reduces contamination due to oppositely-charged leptons from charm decays. Events meeting these criteria are assigned to the **Lepton** category unless the lepton charge and the net charge

of all kaon candidates indicate opposite tags. Events without a lepton tag but with a non-zero net kaon charge are assigned to the **Kaon** category. All remaining events are passed to a neural network algorithm whose main inputs are the momentum and charge of the track with the highest center-of-mass momentum, and the outputs of secondary networks, trained with Monte Carlo samples to identify primary leptons, kaons, and soft pions. Based on the output of the neural network algorithm, events are tagged as B^0 or \bar{B}^0 and assigned to the NT1 (more certain tags) or NT2 (less certain tags) category, or not tagged at all. The tagging power of the NT1 and NT2 categories arises primarily from soft pions and from recovering unidentified isolated primary electrons and muons. The yields, efficiencies, purities and mistag rates w for each tagging category are listed in Table. 1.

Table 1: Event yields for the different tagging categories obtained from fits to the m_{ES} distributions. The purity is quoted for $m_{\text{ES}} > 5.270 \text{ MeV}/c^2$ and average mistag fractions w_i extracted for each tagging category i from the likelihood fit to the time distribution for the fully-reconstructed flavor eigenstate sample.

Category	Tagged	Efficiency (%)	Purity (%)	w
Lepton	754 ± 28	11.3 ± 0.4	97.1 ± 0.6	0.085 ± 0.018
Kaon	2317 ± 54	34.8 ± 0.6	85.2 ± 0.8	0.167 ± 0.014
NT1	556 ± 26	8.3 ± 0.3	88.7 ± 1.5	0.195 ± 0.026
NT2	910 ± 36	13.7 ± 0.4	83.0 ± 1.3	0.326 ± 0.024
Total	4538 ± 75	68.1 ± 0.9	86.7 ± 0.5	

3.5 $B^0\bar{B}^0$ Mixing Result

The value of Δm_d is extracted from the tagged flavor-eigenstate B^0 sample B_{flav} with a simultaneous unbinned likelihood fit to the Δt distributions of both unmixed ($B^0\bar{B}^0$) and mixed (B^0B^0 and $\bar{B}^0\bar{B}^0$) events. The PDFs for the unmixed (+) and mixed (-) signal events for the i^{th} tagging category are given by

$$\mathcal{H}_{\pm}(\Delta t | \Delta m_d, w_i, \hat{a}_i) = \frac{e^{-|\Delta t|/\tau}}{4\tau} [1 \pm (1 - 2w_i) \cos \Delta m_d \Delta t] \otimes \mathcal{R}(\delta_t | \hat{a}_i), \quad (7)$$

Some resolution function parameters are allowed to differ for each tagging category to account for shifts due to inclusion of charm decay products in the tag vertex. The PDFs are extended to include background terms, different for each tagging category. The probability that a B^0 candidate is a signal event is determined from a fit to the observed m_{ES} distribution for its tagging category. The Δt distributions of the combinatorial background are described with a zero lifetime component and a non-oscillatory component with non-zero lifetime. Separate resolution function parameters are used for signal and background to minimize correlations.

The likelihood fit involves a total of 34 parameters, including Δm_d (1), the mistag rates w_i and mistag differences $\Delta w_i = w_i(B^0) - w_i(\bar{B}^0)$ (8), Δt resolution function parameters (9) and background parameters (16). We display the result of the likelihood fit by using the mixing asymmetry,

$$\mathcal{A}_{\text{mix}}(\Delta t) = \frac{N_{\text{unmixed}}(\Delta t) - N_{\text{mixed}}(\Delta t)}{N_{\text{unmixed}}(\Delta t) + N_{\text{mixed}}(\Delta t)}. \quad (8)$$

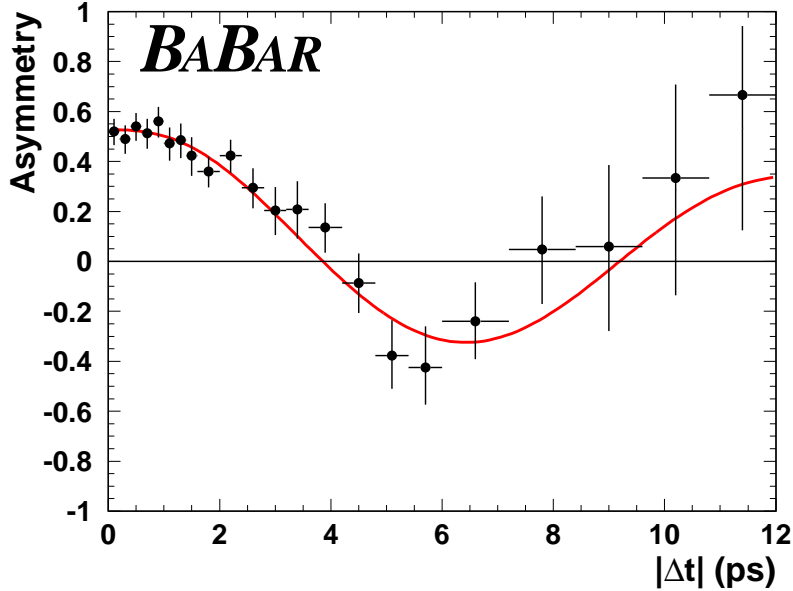


Figure 3: The asymmetry $\mathcal{A}_{mix}(\Delta t)$ between unmixed and mixed events as a function of $|\Delta t|$ overlaid with the result from the likelihood fit.

If flavor tagging and Δt determination were perfect, the asymmetry as a function of Δt would be a cosine with unit amplitude. The amplitude is diluted by mistag probabilities and the Δt resolution. The Δt distributions of mixed and unmixed events, and their asymmetry, \mathcal{A}_{mix} , are shown in Fig. 3.3 and 3.5 along with projections of the fit result. The probability to obtain a smaller likelihood is 28 %.

Systematic uncertainties in the Δm_d measurement arise from various sources. The conversion of Δz to Δt introduces an uncertainty ($\pm 0.007 \text{ ps}^{-1}$) due to the limited knowledge of the PEP-II boost, the z length scale of *BABAR* and the B_{rec} momentum vector in the $\Upsilon(4S)$ frame. Systematic uncertainties related to the resolution function ($\pm 0.005 \text{ ps}^{-1}$), are attributed to the choice of the parameterization, the description of outliers, and the capability of the resolution model to deal with various plausible misalignment scenarios applied to the Monte Carlo simulation. The parameters of the background Δt distribution are left free in the likelihood fit, but systematic errors ($\pm 0.005 \text{ ps}^{-1}$), are introduced by the uncertainty in signal probabilities, parameterization of the background Δt distributions and resolution function, and the small amount of correlated B^+ background. Finally, statistical limitations of Monte Carlo validation tests ($\pm 0.004 \text{ ps}^{-1}$), the full size of a (negative) correction obtained from Monte Carlo ($\pm 0.009 \text{ ps}^{-1}$), and the variation of the B^0 lifetime [4] ($\pm 0.006 \text{ ps}^{-1}$) contribute. These contributions added in quadrature yield a total systematical error of 0.016 ps^{-1} .

In conclusion, the B^0 - \bar{B}^0 mixing frequency Δm_d is determined with a new time-dependent technique from tagged fully-reconstructed B^0 decays to be

$$\Delta m_d = 0.519 \pm 0.020(stat) \pm 0.016(syst) \text{ ps}^{-1}.$$

This preliminary result is one of the single most precise measurements available, and is consistent with the current world average [4] and a recent *BABAR* measurement with a dilepton

sample [10]. The error on Δm_d is still dominated by statistics, leaving substantial room for further improvement as more data are accumulated.

4 Measurement of $\sin 2\beta$

In 32 million $B\bar{B}$, we extract $\sin 2\beta$ from a sample of fully reconstructed B^0 decays (B_{CP}) to final states with $\eta_f = -1$ ($J/\psi K_S^0$, $\psi(2S)K_S^0$, $\chi_{c1}K_S^0$), $\eta_f = +1$ ($J/\psi K_L^0$) and $\eta_f(\text{effective}) = 0.65 \pm 0.07$ ($J/\psi K^{*0}$ with $K^{*0} \rightarrow K_S^0 \pi^0$) [11].

The $\sin 2\beta$ measurement is made with a simultaneous unbinned likelihood fit to the Δt distributions of the tagged B_{CP} and B_{flav} samples. The Δt distribution of the former is given by Eq. 1, with $|\lambda| = 1$. The B_{flav} sample evolves according to the PDF for B^0 flavor oscillations as described in the previous section. The amplitudes for the B_{CP} CP -asymmetries and for the B_{flav} flavor oscillations are reduced by the same factor $(1 - 2w)$ due to wrong tags. Both distributions are convolved with a common Δt resolution function and backgrounds are accounted for by adding terms to the likelihood, incorporated with different assumptions about their Δt evolution and convolved with a separate resolution function. Events are assigned signal and background probabilities based on the m_{ES} (all modes except $J/\psi K_L^0$) or ΔE ($J/\psi K_L^0$) distributions shown in Fig. 4. Separate Δt resolution functions parameters have been used for the data collected in 1999-2000 and 2001, due to the significant improvement in the SVT alignment.

A total of 45 parameters are varied in the likelihood fit, including $\sin 2\beta$ (1), mistag fractions w and differences Δw (8), parameters for the signal Δt resolution (16), and parameters for background time dependence (9), Δt resolution (3) and mistag fractions (8). The determination of the mistag fractions and signal Δt resolution function is dominated by the large B_{flav} sample. The largest correlation between $\sin 2\beta$ and any linear combination of the other free parameters is only 0.13. We fix τ_{B^0} and Δm_d [4].

Figure 4 shows the Δt distributions and A_{CP} as a function of Δt overlaid with the likelihood fit result for the $\eta_f = -1$ and $\eta_f = +1$ samples. The probability of obtaining a lower likelihood is 27%. The simultaneous fit to all CP decay modes and flavor decay modes yields

$$\sin 2\beta = 0.59 \pm 0.14 \text{ (stat)} \pm 0.05 \text{ (syst)}.$$

The dominant sources of systematic error are the parameterization of the Δt resolution function (0.03), due in part to residual uncertainties in SVT alignment, possible differences in the mistag fractions between the B_{CP} and B_{flav} samples (0.03), and uncertainties in the level, composition, and CP asymmetry of the background in the selected CP events (0.02). The systematic errors from uncertainties in Δm_{B^0} and τ_{B^0} and from the parameterization of the background in the B_{flav} sample are small; an increase of 0.020 ps^{-1} in the value for Δm_{B^0} decreases $\sin 2\beta$ by 0.015.

The large sample of reconstructed events allows a number of consistency checks, including separation of the data by decay mode, tagging category and B_{tag} flavor. The results of fits to some subsamples and to the samples of non- CP decay modes are shown in Table 2. For the latter, no statistically significant asymmetry is found.

If $|\lambda|$ is allowed to float in the fit to the $\eta_f = -1$ sample, which has high purity and requires minimal assumptions on backgrounds, we obtain $|\lambda| = 0.93 \pm 0.09 \text{ (stat)} \pm 0.03 \text{ (syst)}$. The sources of systematic error are the same as in the $\sin 2\beta$ analysis.

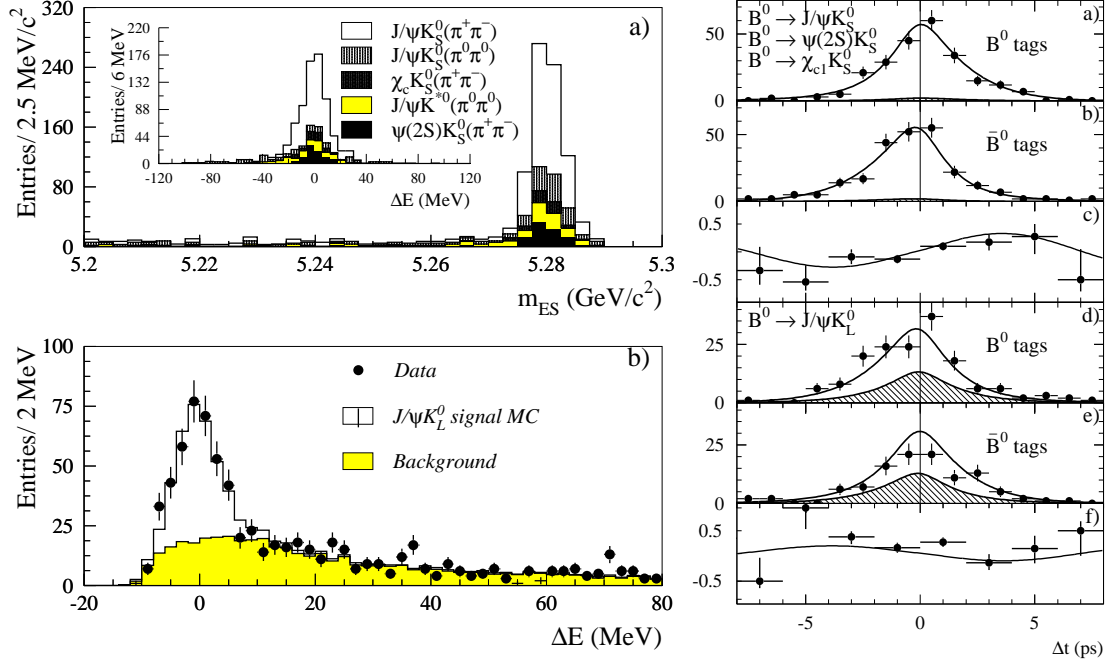


Figure 4: Left: a) distribution of m_{ES} for B_{CP} candidates having a K_S^0 in the final state; b) distribution of ΔE for $J/\psi K_L^0$ candidates. Right: Number of $\eta_f = -1$ candidates ($J/\psi K_S^0$, $\psi(2S)K_S^0$, and $\chi_{c1}K_S^0$) in the signal region a) with a B^0 tag N_{B^0} and b) with a \bar{B}^0 tag $N_{\bar{B}^0}$, and c) the asymmetry $(N_{B^0} - N_{\bar{B}^0})/(N_{B^0} + N_{\bar{B}^0})$, as functions of Δt . The solid curves represent the result of the combined fit to all selected CP events; the shaded regions represent the background contributions. Figures d)–f) contain the corresponding information for the $\eta_f = +1$ mode ($J/\psi K_L^0$).

Table 2: Number of tagged events, signal purity and observed CP asymmetries in the CP samples and control samples. Errors are statistical only.

Sample	N_{tag}	Purity (%)	$\sin 2\beta$
$J/\psi K_S^0, \psi(2S)K_S^0, \chi_{c1}K_S^0$	480	96	0.56 ± 0.15
$J/\psi K_L^0$	273	51	0.70 ± 0.34
$J/\psi K^{*0}, K^{*0} \rightarrow K_S^0 \pi^0$	50	74	0.82 ± 1.00
Full CP sample	803	80	0.59 ± 0.14
B_{flav} non- CP sample	7591	86	0.02 ± 0.04
Charged B non- CP sample	6814	86	0.03 ± 0.04

The measurement of $\sin 2\beta = 0.59 \pm 0.14$ (stat) ± 0.05 (syst) establishes CP violation in the B^0 meson system at the 4.1σ level. This significance is computed from the sum in quadrature of the statistical and additive systematic errors. The probability of obtaining this value or higher in the absence of CP violation is less than 3×10^{-5} . The corresponding probability for the $\eta_f = -1$ modes alone is 2×10^{-4} .

5 Measurement of $\sin 2\alpha$

We reconstruct neutral B mesons decaying to $h^+h'^-$, where h and h' refer to π or K in a sample of 33 million $B\bar{B}$. The data set includes 30.4fb^{-1} collected on the $\Upsilon(4S)$ resonance and 3.3fb^{-1} collected below the $B\bar{B}$ threshold used for continuum background studies.

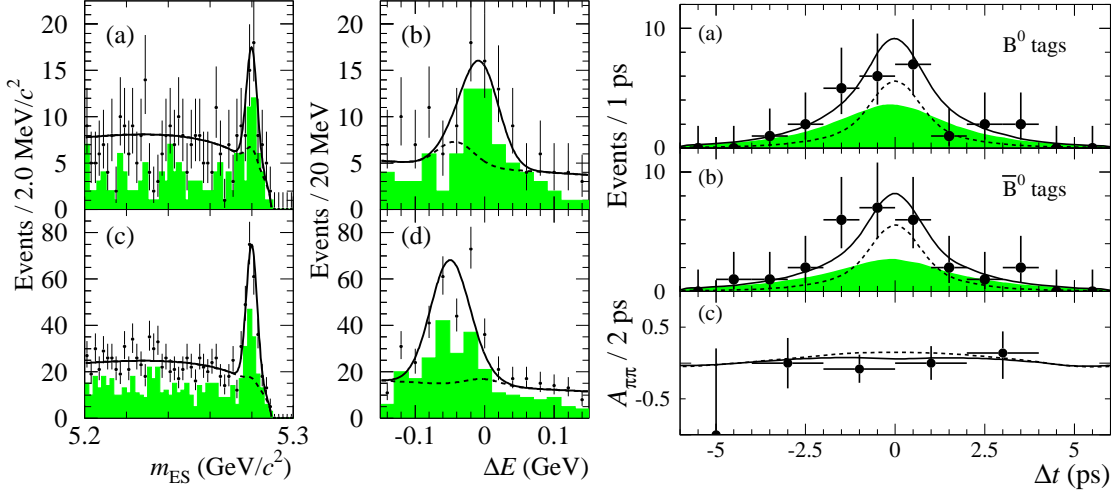


Figure 5: Left: Distributions of m_{ES} and ΔE (unshaded histograms) for events enhanced in signal (a), (b) $\pi\pi$ and (c), (d) $K\pi$ decays. Solid curves represent projections of the maximum likelihood fit result, while dashed curves represent $q\bar{q}$ and $\pi\pi \leftrightarrow K\pi$ cross-feed background. Shaded histograms show the subset of events that are tagged. Right: Distributions of Δt for events enhanced in signal $\pi\pi$ decays. Figures (a) and (b) show events (points with errors) with $B_{\text{tag}} = B^0$ or \bar{B}^0 . Solid curves represent projections of the likelihood fit, dashed curves represent the sum of $q\bar{q}$ and $K\pi$ background, and the shaded region represents the contribution from signal $\pi\pi$. Figure (c) shows $\mathcal{A}_{\pi\pi}(\Delta t)$ for data (points with errors), as well as fit projections for signal and background (solid curve), and signal only (dashed curve).

We select $B \rightarrow h^+h'^-$ candidates in the region $5.2 < m_{\text{ES}} < 5.3\text{ GeV}/c^2$ and $|\Delta E| < 0.15\text{ GeV}$ and apply requirements on track multiplicity and event topology. The total number of events satisfying these criteria is 9741. This sample contains 97% background, mostly due to random combinations of tracks produced in $e^+e^- \rightarrow q\bar{q}$ events. We extract signal and background yields for $\pi^+\pi^-$, $K^+\pi^-$, and K^+K^- decays, and the amplitudes of the $\pi\pi$ sine ($S_{\pi\pi}$) and cosine ($C_{\pi\pi}$) oscillation terms simultaneously from an unbinned likelihood fit. We parameterize the $K\pi$ component in terms of the total yield and the CP -violating charge asymmetry $\mathcal{A}_{K\pi} \equiv (N_{K^-\pi^+} - N_{K^+\pi^-}) / (N_{K^-\pi^+} + N_{K^+\pi^-})$. Background parameters are determined from m_{ES} and ΔE sideband regions.

Discrimination between signal and background is based on m_{ES} , ΔE , and a Fisher discriminant \mathcal{F} [12] constructed from the scalar sum of the CM momenta of tracks and photons (excluding tracks from the B_{rec} candidate) and between pions and kaon tracks on the Cherenkov angle measurement from the DIRC. The inclusion of events with no flavor tag improves the signal yield estimates and provides a larger sample for determining background shape parameters in the likelihood fit.

There are 18 free parameters in the fit. In addition to the CP -violating parameters $S_{\pi\pi}$, $C_{\pi\pi}$, and $\mathcal{A}_{K\pi}$ (3), the fit determines signal and background yields (6), the background $K\pi$ charge asymmetry (1), and parameters describing the background shapes in m_{ES} , ΔE , and \mathcal{F} (8). We fix τ and Δm_d [4]. The Δt PDF for signal $\pi^+\pi^-$ decays is given by Eq. 1, modified to include mistags and convolved with the signal resolution function. The Δt PDF for signal $K\pi$ events takes into account $B^0-\bar{B}^0$ mixing and $B^0 \rightarrow K^+K^-$ decays are parameterized as an exponential convolved with the resolution function.

Figure 5 shows distributions of m_{ES} and ΔE for events enhanced in signal decays based on likelihood ratios and the Δt distributions and CP asymmetry $\mathcal{A}_{\pi\pi}(\Delta t) = (N_{B^0}(\Delta t) - N_{\bar{B}^0}(\Delta t))/(N_{B^0}(\Delta t) + N_{\bar{B}^0}(\Delta t))$ for tagged events enhanced in signal $\pi\pi$ decays (approximately 24 $\pi\pi$, 22 $q\bar{q}$, and 5 $K\pi$ events satisfy this selection).

In conclusion, in a sample of 33 million $B\bar{B}$, we find 65_{-11}^{+12} $\pi\pi$, 217 ± 18 $K\pi$, and $4.3_{-4.3}^{+6.3}$ KK events. These yields are consistent with the branching fractions reported in Ref. [12]. We measure the following CP parameters:

$$\begin{aligned} S_{\pi\pi} &= 0.03_{-0.56}^{+0.53} \text{ (stat)} \pm 0.11 \text{ (syst)}, & \mathcal{A}_{K\pi} &= -0.07 \pm 0.08 \text{ (stat)} \pm 0.02 \text{ (syst)}, \\ C_{\pi\pi} &= -0.25_{-0.47}^{+0.45} \text{ (stat)} \pm 0.14 \text{ (syst)}. \end{aligned}$$

The correlation between $S_{\pi\pi}$ and $C_{\pi\pi}$ is -21% , while $\mathcal{A}_{K\pi}$ is uncorrelated with $S_{\pi\pi}$ and $C_{\pi\pi}$. Systematic errors on $S_{\pi\pi}$, $C_{\pi\pi}$, and $\mathcal{A}_{K\pi}$ arise primarily from uncertainties in PDF shapes, tagging efficiencies and dilutions, τ , and Δm_d .

6 Summary and Outlook

We have observed CP violation in the neutral B system at the 4.1σ level using a sample of fully reconstructed B^0 decays to CP eigenstates. With the same novel technique of time-dependent measurements, we have determined the B^+ and B^0 lifetimes and the $B^0\bar{B}^0$ mixing frequency Δm_d with high precision. In addition, we have presented the first measurement of the time-dependent asymmetry in $B^0 \rightarrow \pi^+\pi^-$ decays. All results are limited by the data sample size and we expect improved measurements from the rapidly growing *BABAR* data sample in the near future especially for the CP violating asymmetries.

References

- [1] J.H. Christenson *et al.* Phys. Rev. Lett. **13**, 138 (1964).
- [2] N. Cabibbo, Phys. Rev. Lett. **10**, 531 (1963);
M. Kobayashi and T. Maskawa, Prog. Th. Phys. **49**, 652 (1973).
- [3] A.B. Carter and A.I. Sanda, Phys. Rev. **D23**, 1567 (1981);
I.I. Bigi and A.I. Sanda, Nucl. Phys. **B193**, 85 (1981).
- [4] Particle Data Group, D.E. Groom *et al.*, Eur. Phys. Jour. C **15**, 1 (2000).
- [5] See, for example, L. Wolfenstein, Eur. Phys. Jour. C **15**, 115 (2000).

- [6] M. Beneke, G. Buchalla, M. Neubert, and C.T. Sachrajda, Nucl. Phys. B **606**, 245 (2001);
Y.Y. Keum, H-n. Li, and A.I. Sanda, Phys. Rev. D **63**, 054008 (2001);
M. Ciuchini *et al.*, Phys. Lett. B **515**, 33 (2001).
- [7] *BABAR* Collaboration, B. Aubert *et al.*, *BABAR-PUB-01/08*, to appear in Nucl. Instrum. Methods.
- [8] G.C. Fox and S. Wolfram, Phys. Rev. Lett. **41**, 1581 (1978).
- [9] *BABAR* Collaboration, B. Aubert *et al.* Phys. Rev. Lett. **87**, 201803 (2001).
- [10] T. Brandt, contribution to this conference.
- [11] *BABAR* Collaboration, B. Aubert *et al.* Phys. Rev. Lett. **86**, 2515 (2001);
BABAR Collaboration, B. Aubert *et al.* Phys. Rev. Lett. **87**, 091801 (2001).
- [12] *BABAR* Collaboration, B. Aubert *et al.*, Phys. Rev. Lett. **87**, 151802 (2001).